J. Am. Ceram. Soc., 96 [1] 32–36 (2013)
DOI: 10.1111/jace.12090

journal
Rapid Communication

Reactive Hot Pressing of ZrC–SiC Ceramics at Low Temperature

Xin-Gang Wang, Guo-Jun Zhang,*,† Jia-Xiang Xue, Yun Tang, Xiao Huang, Chang-Ming Xu, and Pei-Ling Wang

State Key Laboratory of High Performance Ceramics and Superfine Microstructures, Shanghai Institute of Ceramics, Shanghai 200050, China

Composites of ZrC–SiC with relative densities in excess of 98% were prepared by reactive hot pressing of ZrC and Si at temperature as low as 1600°C. The reaction between ZrC and Si resulted in the formation of ZrC_{1-x}, SiC, and ZrSi. Low-temperature densification of ZrC−SiC ceramics is attributed to the formed nonstoichiometric ZrC_{1-x} and Zr–Si liquid phase. Adding 5 wt% Si to ZrC, the three-point bending strength of formed $ZrC_{0.8}$–13.4 vol%SiC ceramics reached 819 ± 102 MPa with hardness and toughness being 20.5 GPa and 3.3 MPa·m$^{1/2}$, respectively.

I. Introduction

Zirconium carbide is an important member in the family of ultra-high temperature ceramics duo to its high melting point, high hardness, good thermal shock resistance, and solid-state phase stability.[1,2] Consequently, ZrC could be a good potential material for structural components used in next-generation rocket engines and hypersonic spacecraft.[3] In addition, ZrC is being considered as one of the possible materials for the inert matrix fuels (IMF) in the generation-IV nuclear reactor systems, due to its excellent neutronic and high-temperature mechanical properties as well as resistance to corrosion by fission products.[4,5] During the preparation of IMF, low temperature is generally needed to maintain the stability of fuels and avoid the reaction between the matrix and the fuel materials.[6] However, ZrC has poor sinterability, mainly owing to its strong covalent bond and low self-diffusion coefficient. In general, pressure-assisted techniques and high sintering temperatures (>2000°C) are applied to obtain dense ZrC bodies by hot pressing from commercially available powders.[7] Without any sintering aids, ZrC ceramics with relative density ranging from 94% to 97% can be obtained by hot pressing under 30–40 MPa pressures at temperatures higher than 2200°C.[8,9] To reduce the sintering temperature required for densification of ZrC, metal and nonmetal sintering aids such as Nb, $MoSi_2$, and VC have been chosen.[2,10,11]

In addition to the additive approach that is commonly used to obtain dense ZrC-based ceramics, reactive hot pressing (RHP) is another way to obtain high-density ceramics, which has an advantage of producing ceramics at reduced temperatures compared with non-reactive processes.[12,13] ZrC ceramics prepared by RHP method using Zr and C as raw powders has been reported.[14] The results showed that nearly fully dense ZrC with fine grains was obtained at temperatures as low as 1200°C–1600°C. The addition of SiC to form ZrC–SiC composites enhances the sinterability of ZrC ceramics and results in ZrC–SiC composites with improved mechanical properties.[15] However, the research studies dealing with reactive hot pressing of ZrC–SiC composites have been very few. In this work, the investigation of ZrC–SiC composites fabricated by reactive hot pressing (RHP) using ZrC and Si as starting materials was carried out. The reaction process and the densification behavior during the RHP were also discussed.

II. Experimental Procedure

The starting powders were ZrC (99% purity, 0.5–3 μm,) and Si (>99% purity, <50 μm; Yinfeng Silcon Co. Ltd., Jinan, China), in which ZrC was synthesized by carbothermal reduction as described in the previous work.[11] To decrease the particle size of Si, the powder was milled for 8 h using Si_3N_4 balls as the milling medium to obtain a final particle size of about 1–3 μm. ZrC without and with different content (2.5, 5.0, 10 wt%) of Si were mixed by mixing in ethanol for 24 h in a plastic bottle and the corresponding samples were designated as ZS0, ZS2.5, ZS5, and ZS10, respectively. A rotary evaporator was used to remove the ethanol at 70°C. The powder mixtures were sieved to 200 mesh. The powders were then compacted in a graphite die lined with a graphite foil and coated with BN. The compacts were hot-pressed at temperatures ranging from 1300°C to 2000°C in 100°C increments to produce samples with dimensions of 22 mm in diameter for investigation of the reaction process and densification behavior. Rectangular samples with dimensions of 37 mm (length) × 30 mm (width) × 5 mm (high) were prepared for mechanical properties measurements. A heating rate of 20°C/min was used and a pressure of 40 MPa was applied from 1350°C. The atmosphere was vacuum (<10 Pa) under 1000°C and then switched to flowing argon. After holding at soaking temperatures for 60 min, the applied pressure was removed and the furnace was cooled naturally to room temperature. The bulk densities of sintered ceramics were measured using the Archimedes method. The final relative densities were determined as the ratio of experimental bulk densities to theoretical ones calculated from the rule of mixtures based on the final phase content according to XRD analysis results at 1600°C. The theoretical density of ZrC_{1-x} from reference,[16] ZrSi (5.66 g/cm^3) from JCPDS Card 72-2031, and SiC (3.21 g/cm^3) from JCPDS Card 75-0254 were used to calculate the theoretical densities of the obtained ZrC-based ceramics. Phase composition was determined by X-ray diffraction (XRD; D/max 2550 V, Rigaku Co., Tokyo, Japan). The XRD profiles of the products were recorded through a Huber G670 imaging plate Guinier camera ($CuK_{\alpha 1}$, Ge monochromator, 40 KV, 30 mA) with internal standard LaB_6 (λ = 4.15692 Å). The lattice parameters of ZrC phase were determined by indexing and least-squares refinement with the MDI Jade5.0 software.[17] The microstructure

G. Hilmas—contributing editor

Manuscript No. 31633. Received June 25, 2012; approved October 18, 2012.
*Member, The American Ceramic Society
†Author to whom correspondence should be addressed. e-mail: gjzhang@mail.sic.ac.cn

of fracture surfaces was observed by scanning electron microscopy (SEM; Hitachi S-570, Hitachi Ltd., Tokyo, Japan) in secondary electron mode. The backscattered electron (BSE) images were obtained by electron probe microanalyzer (JXA-8100F, JEOL, Japan). Before the observation, the samples were polished with a diamond paste to 0.5 μm. The chemical compositions of polished surfaces were then analyzed with energy-dispersive spectroscopy (EDS, Oxford INCA energy) that was linked to the electron probe microanalyzer. Quantitative analyses of phases were done using Image pro Plus 5.0 program. The hardness was measured by the Vickers indentation method (Instron Wilson-Wolpert Tukon 2100B, Instron Co., Norwood, MA) using a load of 9.8 N and a dwell time of 15 s on a polished surface. The indentation fracture toughness was calculated according to the equation of Evans.[18,19] The values of hardness and fracture toughness were based on an average of five measurements for each specimen. Flexural strength was examined by a three-point bending test on bars with dimensions of 2 mm × 2.5 mm × 25 mm. The testing span and crosshead speed used were 20 mm and 0.5 mm/min, respectively. The average flexural strength of ZS5 was obtained based on the measurements of six bars.

III. Results and Discussion

The variation of the relative densities for ZS0, ZS2.5, ZS5, and ZS10 with sintering temperatures is shown in Fig. 1(a). It is noted that the relative densities of ZS5 and ZS10 sintered at 1600°C and 1700°C are very close (98% and 99%, respectively) and much higher than that of ZS0 and ZS2.5 at the same temperatures. There is a remarkable jump in relative density of ZS5 and ZS10 when the sintering temperatures are increased from 1500°C to 1600°C, which is well agreed with the shrinkage of samples during hot-pressing processes presented by displacement curves versus sintering time under different temperatures, as shown in Fig. 1(b). For ZS0 and ZS2.5, the increase in sintering temperature does not make the samples fully dense, as the relative densities of ZS0 and ZS2.5 are less than 83% and 95% even after sintering at 1800°C and 2000°C, respectively, as shown in Fig. 1(a). The relative density changes can also be confirmed by the microstructure images. The fracture surface of ZS5 and ZS10 sintered at 1500°C and 1600°C are shown in Fig. 2. A large amount of small pores can be found on the fracture surface of ZS5 [Fig. 2(a)] and ZS10 [Fig. 2(c)] sintered at 1500°C, while the grains are homogeneously distributed with average size less than 1 μm for both samples. For increasing the sintering temperature to 1600°C, almost no pores can be found from the microstructures of both ZS5 and ZS10, as shown in Figs. 2(b) and (d), respectively, which is in accordance with the relative density data as mentioned above.

X-Ray Diffraction patterns of the ZS5 and ZS10 sintered at different temperatures are shown in Fig. 3. The disappearance of Si diffraction peaks in XRD patterns of ZS5 sintered at 1300°C, as shown in Fig. 3(a), implies that the reaction between ZrC and Si occurred starting from below this temperature. On the other hand, ZrSi was detected in ZS5 and ZS10 sintered at 1300°C, whose intensities of XRD peaks decreased a little bit with the increase in temperature up to 1600°C, especially for ZS5. The second phase β-SiC (JCPDS Card 65-0360) was identified clearly in both ZS5 and ZS10 sintered at 1500°C and 1600°C, while the XRD peak intensity of β-SiC increased from 1500°C to 1600°C. According to the results of phase identification of ZS5 and ZS10, the reactions between ZrC and Si could be assumed as the following two processes. First, part of ZrC reacted with Si to form ZrSi and SiC. With the increase in temperature, carbon atom from the other part of ZrC diffused into ZrSi phase to form ZrC_{1-x} and SiC. The assumption could be confirmed by the determination of lattice parameter and microstructure analyses. The lattice parameter of ZrC in ZS5 and ZS10 sintered at 1300°C is 4.697(3) and 4.696(2) Å, respectively (see Table I, the values in the parenthesis represent the standard deviation of the lattice parameter), which is about the same as that of the raw ZrC powders (4.697(1) Å), revealing that the carbon defect concentration in ZrC_{1-x} lattice was very low. With the sintering temperature increase up to 1500°C, the lattice parameters of ZrC_{1-x} in ZS5 and ZS10 decease to 4.695(1) and 4.693(1) Å, respectively, implying the formation

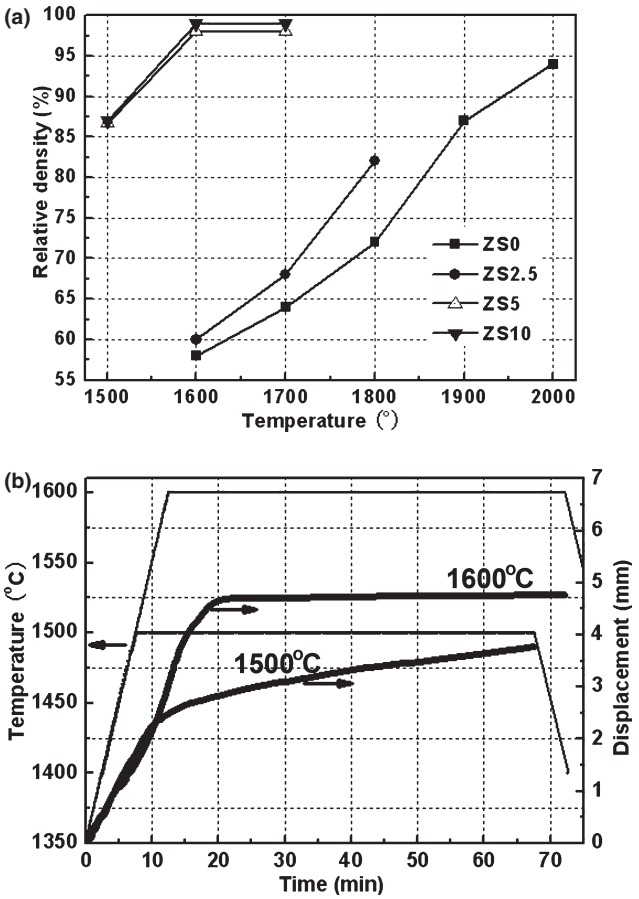

Fig. 1. The relative density versus sintering temperature of ZrC–SiC–based ceramics (a) and the displacement curves of the punch of ZS10 versus sintering time at 1500°C and 1600°C (b).

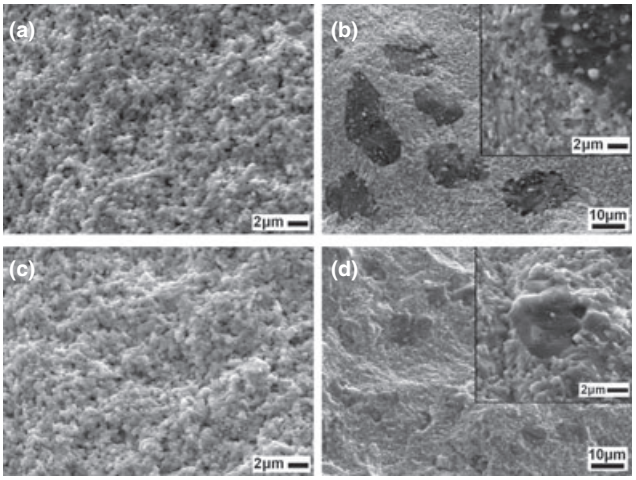

Fig. 2. The fracture surface of ZS5 and ZS10 sintered at different temperatures. (a) ZS5°C–1500°C, (b) ZS5°C–1600°C, (c) ZS10°C–1500°C, (d) ZS10°C–1600°C.

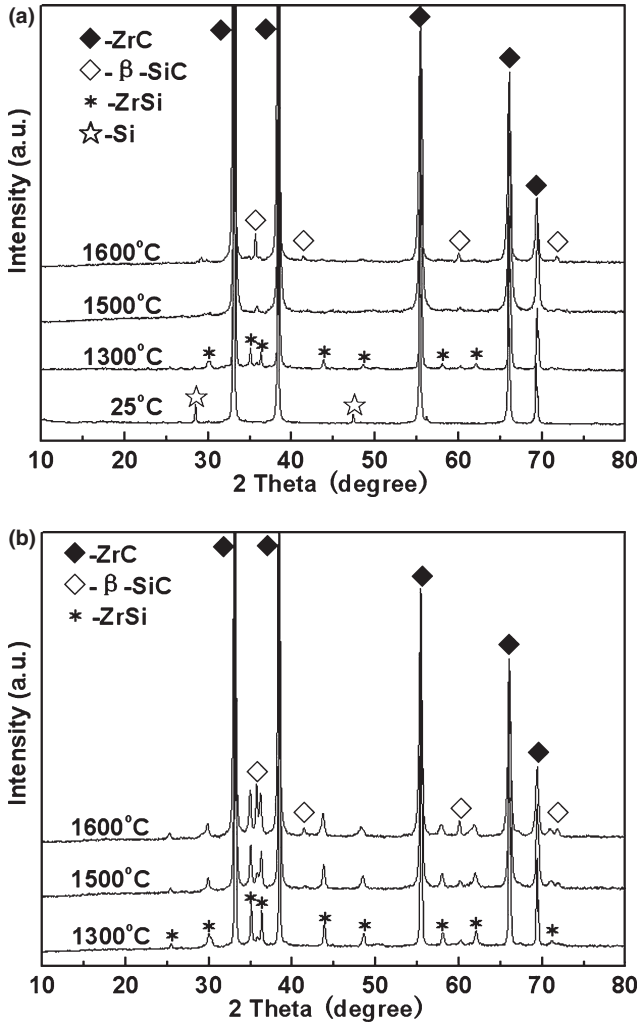

Fig. 3. XRD patterns of ZS5 (a) and ZS10 (b) sintered at the different temperatures.

Table I. The Lattice Parameters of ZS5 and ZS10 at Different Temperatures

	Lattice parameters (Å) of ZrC_{1-x}		
Sample	at 1300°C	at 1500°C	at 1600°C
ZS5	4.697(3)†	4.695(1)	4.688(1)
ZS10	4.696(2)	4.693(1)	4.688(1)

†The values in the parentheses represent the standard deviation of the lattice parameters of ZrC_{1-x}.

of ZrC_{1-x}. For ZS5 and ZS10 sintered at 1600°C, the lattice parameter of ZrC_{1-x} both decrease to 4.688(1) Å, which is corresponding to that of $ZrC_{0.8}$, (4.687 Å).[9] The carbon defect concentration changes in ZS5 and ZS10 could confirm the formation of nonstoichiometric ZrC_{1-x} in reaction process.

The BSE images of polished surfaces for ZS5 and ZS10 and their EDS analysis are shown in Fig. 4. The phase with light color is ZrC_{1-x} matrix, while the phase with 2–15 μm grains and dark color is SiC. The ZrSi phase with gray color can be seen in the BSE image for sample ZS10 [Fig. 4(b)]. From the polished surface of ZS5 and ZS10, it can be found that some small grains (particle size less than 1.0 μm) existed in the SiC grains. According to the image contrast and the EDS line-scanning analysis (Fig. 5), the larger particles (average size about 0.5–1.0 μm) with high Zr content and low Si content inside the SiC grains should be ZrC_{1-x}. The smaller

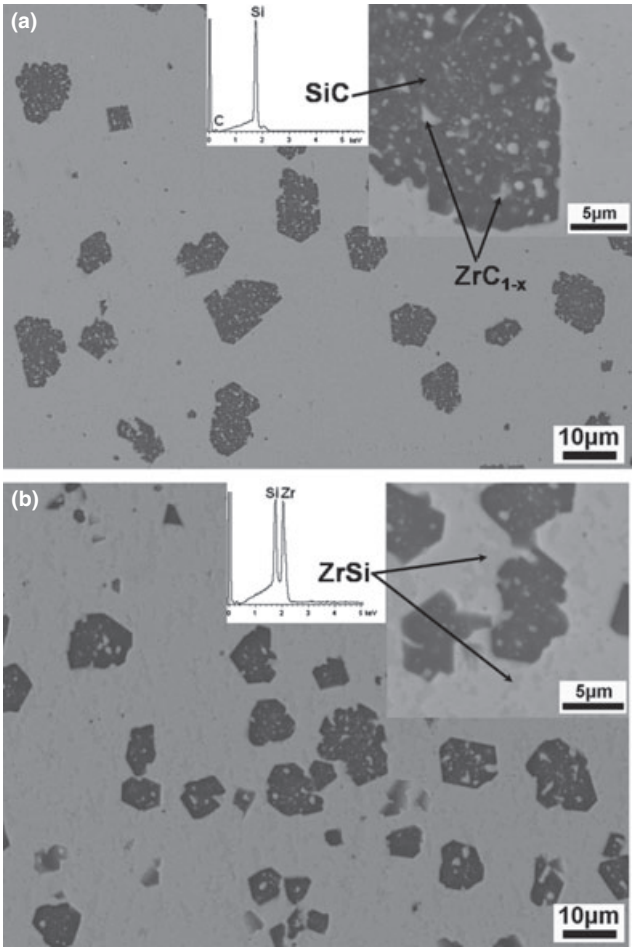

Fig. 4. The polished surface of ZS5 (a), ZS10 (b) sintered at 1600°C, and EDS spectra.

particles (average size about less than 500 nm) inside SiC grains should be the same with the large ones, but probably include some amount of residual ZrSi. In addition, it is noticed that the amount of ZrSi in the samples is affected by the Si content in the starting composition. For Si content of less than 5 wt%, only a trace of ZrSi could be formed, as shown in Fig. 4(a), indicating that almost all the ZrSi reacted with ZrC to form ZrC_{1-x} and SiC. According to the theoretical calculation that if all the added Si reacted with ZrC in ZS2.5 and ZS5, the final composition of the obtained ceramics would be $ZrC_{0.9}$–7.5 vol%SiC and $ZrC_{0.8}$–13.4 vol% SiC, respectively. With an increase in the Si content up to 10 wt %, the ZrSi content increased to greater than 10 vol%. The mass fraction of the ZrSi phase in ZS10 was calculated by using the *K* value method based on the relative intensity of the strongest diffraction peak of ZrC and ZrSi and then converted to volume fraction.[20] The final composites of ZS10 sintered at 1600°C was $ZrC_{0.8}$–16.7 vol% SiC–10.9 vol% ZrSi. The image analysis method was also used to quantify the phase content of ZS5 and ZS10 and the results were shown in Table II. The final composition of ZS5 was $ZrC_{0.8}$–10.0 vol%SiC–2.6 vol%ZrSi, while the composition of ZS10 was $ZrC_{0.8}$–14.5 vol%SiC–13.2 vol%ZrSi. It indicates that there is still 2.6 vol% ZrSi in ZS5 sample sintered at 1600°C, which is in accordance with the phase diagram of Zr–Si–C,[21] although it is difficult for XRD method to detect such a trace of ZrSi.

From the phase evolutions, the densification improvement of ZrC with Si addition was owing to the formation of nonstoichiometric ZrC_{1-x}. Based on our previous work,[16] the densification of ZrC was affected by the carbon defects in the ZrC lattice, which not only promoted mass transfer

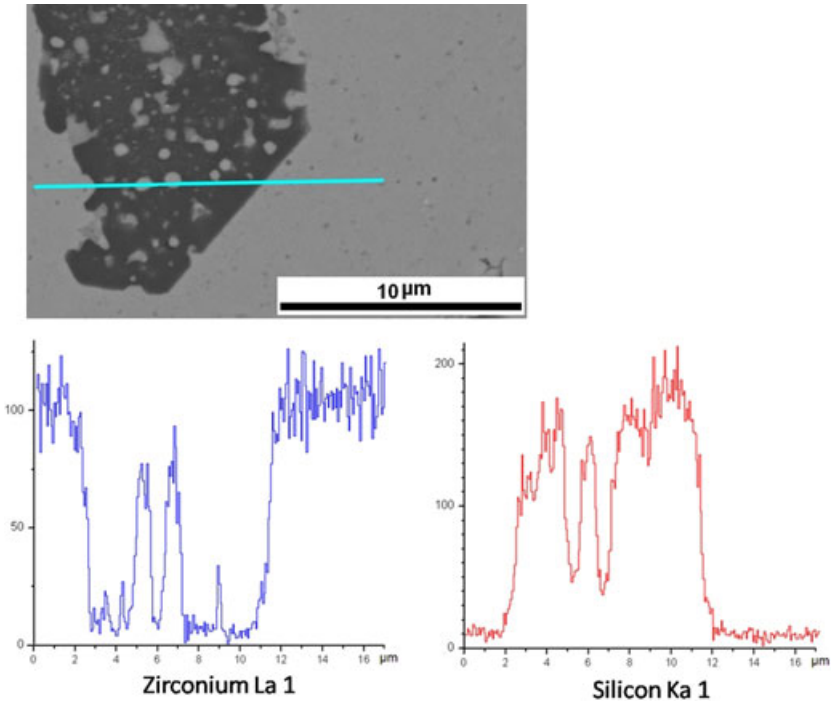

Fig. 5. The EDS line-scanning analysis of ZS5 showing the distribution of Zr and Si elements.

Table II. The Phase Content by XRD Analysis and Image Analysis, and the Mechanical Properties of ZS5 and ZS10

	XRD analysis (vol%)		Image analysis (vol%)				
Samples	SiC	ZrSi	SiC	ZrSi	Hv1.0 (GPa)	K_{IC} (MPa·m$^{1/2}$)	σ (MPa)
ZS5	13.4	trace	10.0	2.6	20.5 ± 1.0	3.3 ± 0.1	819 ± 102
ZS10	16.7	10.9	14.5	13.2	19.0 ± 0.5	2.9 ± 0.3	—

through solid-state diffusion but also had the advantage of accelerating plastic flow during the hot-pressing processes. Meanwhile, the existence of the ZrSi phase also has the advantage of improving the densification. According to the phase diagram of Si–Zr,[22] a liquid phase containing Zr and Si could appear at about 1630°C, which was close to the densification temperature (1600°C) when considering the infrared measurement error of temperature (20°C–30°C). It seems that the molten ZrSi phase aggregated together to form large ZrSi particles first, and then carbon from the ZrC matrix diffused into these particles to form SiC and ZrC_{1-x}. The formed liquid phase should have enhanced the rearrangement of ZrC particles, improved the densification behavior, and also promoted the growth of SiC grains. The detail of the microstructure formation mechanism is an interesting issue, and it would be investigated in the future work.

The mechanical properties of ZS5 and ZS10 were preliminarily evaluated and shown in Table II. Due to the lower hardness of ZrSi (about 10 GPa)[23] compared with that of ZrC and SiC, the hardness of ZS10 (19.0 ± 0.5 GPa) was a little lower than that of ZS5 (20.5 ± 1.0 GPa). The hardness of low-temperature (1600°C) sintered ZS5 and ZS10 was comparable to those of monolithic ZrC sintered at 1900°C–2000°C (about 20 GPa).[2,20] The fracture toughness of ZS5 (3.3 ± 0.1 MPa·m$^{1/2}$) and ZS10 (2.9 ± 0.3 MPa·m$^{1/2}$) were higher than those monolithic ZrC (1.9 ± 0.4 MPa·m$^{1/2}$) and close to the ZrC with addition of 9 vol% $MoSi_2$ (3.3 ± 0.4 MPa·m$^{1/2}$)[2]. The three-point bending strength of ZS5 was 819 ± 102 MPa, which was much higher than that (390 MPa) of ZrC–20 vol%SiC composites (ZrC grain size > 10 μm, SiC grain size < 2 μm) by hot pressing,[15] probably owing to the fine grain size (<2 μm) of the matrix ZrC. Although the SiC grains were in large size, the strength behavior of ZS5 would not be poor, especially with the existence of inside submicrometer-sized ZrC particles. The strength of the obtained ZrC–SiC composites might be mainly controlled by the grain size of the ZrC matrix, but further investigation should be done to verify it.

IV. Summary

ZrC–SiC composites were prepared by reactive hot pressing at temperatures up to 1600°C using ZrC and Si as raw material. The lattice parameter and microstructure analyses confirmed that carbon from the ZrC reacted with Si to form ZrSi and SiC above 1300°C, with an increase in temperature up to 1600°C, carbon atoms from remaining ZrC diffused into the ZrSi phase to form ZrC_{1-x} and SiC. The carbon defects in the final ZrC_{1-x} matrix, and part of the reaction product of ZrSi, promoted the densification of ZrC-based ceramics. The low-temperature sintered ZrC–SiC ceramics (ZS5) had a Vickers hardness and fracture toughness of 20.5 ± 1.0 GPa and 3.3 ± 0.1 MPa·m$^{1/2}$, respectively, which were comparable to the literature results. The bending strength of ZS5 was as high as 819 ± 102 MPa.

Acknowledgments

Financial supports from the Chinese Academy of Sciences under the Program for Recruiting Outstanding Overseas Chinese (Hundred Talents Program), the National Natural Science Foundation of China (No. 91 026 008, 11 175 228 and 11 205 229), and the State Key Laboratory of High Performance Ceramics and Superfine Microstructures are greatly appreciated.

References

[1]K. Upadhya, J. M. Yang, and W. P. Hoffman, "Materials for Ultra High Temperature Structural Applications," *Am. Ceram. Soc. Bull.*, **76** [12] 51–6 (1997).

[2]D. Sciti, S. Guicciardi, and M. Nygren, "Spark Plasma Sintering and Mechanical Behaviour of ZrC-Based Composites," *Scripta Mater.*, **59** [6] 638–41 (2008).

[3]Y. G. Wang, Q. M. Liu, J. L. Liu, L. T. Zhang, and L. F. Cheng, "Deposition Mechanism for Chemical Vapor Deposition of Zirconium Carbide Coatings," *J. Am. Ceram. Soc.*, **91** [4] 1249–52 (2008).

[4]G. Vasudevamurthy, T. W. Knight, E. Roberts, and T. M. Adams, "Laboratory Production of Zirconium Carbide Compacts for Use in Inert Matrix Fuels," *J. Nucl. Mater*., **374** [1–2] 241–7 (2008).

[5]D. Gosset, M. Dolle, D. Simeone, G. Baldinozzi, and L. Thome, "Structural Evolution of Zirconium Carbide Under Ion Irradiation," *J. Nucl. Mater*., **373** [1–3] 123–9 (2008).

[6]C. Shih, J. S. Tulenko, and R. H. Baney, "Low-Temperature Synthesis of Silicon Carbide Inert Matrix Fuel Through a Polymer Precursor Route," *J. Nucl. Mater*., **409** [3] 199–206 (2011).

[7]P. Barnier, C. Brodhag, and F. Thevenot, "Hot-Presing Kinetics of Zirconium Carbide," *J. Mater. Sci*., **21**, 2547–52 (1986).

[8]V. P. Bulychev, R. A. Andrievskii, and L. B. Nezhevenko, "The Sintering of Zirconium Carbide," *Powder Metall. Met. Ceram*., **16** [4] 273–6 (1977).

[9]G. V. Samsonov, M. S. Koval'chenko, R. Y. Petrykina, and V. Y. Naumenko, "Hot Pressing of the Transition Metals and Their Carbides in Their Homogeneity Regions," *Powder Metall. Met. Ceram*., **9** [9] 713–6 (1970).

[10]W. G. Lidman, and H. J. Hamjian, "Reactions During Sintering of a Zirconium Carbide-Niobium Cermet," *J. Am. Ceram. Soc*., **35** [9] 236–40 (1964).

[11]X. G. Wang, J. X. Liu, Y. M. Kan, and G. J. Zhang, "Effect of Solid Solution Formation on Densification of Hot-Pressed ZrC Ceramics with MC (M=V, Nb, and Ta) Additions," *J. Euro. Ceram. Soc*, **32** [8] 1795–802 (2012).

[12]A. L. Chamberlain, W. G. Fahrenholtz, and G. E. Hilmas, "Low-Temperature Densification of Zirconium Diboride Ceramics by Reactive Hot Pressing," *J. Am. Ceram. Soc*., **89** [12] 3638–45 (2006).

[13]W. W. Wu, G. J. Zhang, Y. M. Kan, and P. L. Wang, "Reactive Hot Pressing of ZrB_2-SiC-ZrC Composites at 1600 degrees C," *J. Am. Ceram. Soc*., **91** [8] 2501–8 (2008).

[14]C. Nachiappan, L. Rangaraj, C. Divakar, and V. Jayaram, "Synthesis and Densification of Monolithic Zirconium Carbide by Reactive Hot Pressing," *J. Am. Ceram. Soc*., **93** [5] 1341–6 (2010).

[15]B. Ma, X. Zhang, J. Han, and W. Han, "Fabrication of Hot-pressed ZrC-Based Composites," *Proceedings of the Institution of Mechanical Engineers Part G J.Aero. Eng*, **223** [G8] 1153–7 (2009).

[16]X. Wang, W. Guo, Y. Kan, G. Zhang, and P. Wang, "Densification Behavior and Properties of Hot-Pressed ZrC Ceramics with Zr and GraphiteAdditives," *J. Euro. Ceram. Soc*, **31** [6] 1103–11 (2011).

[17]Materials Data JADE Release 5, "XRD Pattern Processing." Materials Data Inc.(MDI), 1999.

[18]A. G. Evans, and E. A. Charles, "Fracture Toughness Determinations by Indentation," *J. Am. Ceram. Soc*., **59** [7–8] 371–2 (1976).

[19]X. G. Wang, W. M. Guo, Y. M. Kan, and G. J. Zhang, "Hot-Pressed ZrB_2 Ceramics With Composite Additives of Zr and B_4C," *Adv. Eng. Mater*., **12** [9] 893–8 (2010).

[20]D. W. Ni, G. J. Zhang, Y. M. Kan, and P. L. Wang, "Synthesis of Monodispersed Fine Hafnium Diboride Powders Using Carbo/borothermal Reduction of Hafnium Dioxide," *J. Am. Ceram. Soc*., **91** [8] 2709–12 (2008).

[21]ACerS-NIST Phase Equilibria Diagram. CD-ROM Database, Version 3.1, 2005

[22]H. Okamoto, "The Si-Zr (Silicon-Zirconium) System," *J.Phase Equilib*, **11** [5] 513–9 (1990).

[23]W. Martienssen and H. Warlimont, *Springer Handbook of Condensed Matter and Materials Data*. Springer, Berlin Heidelberg, 2005. □